

AN ANALOG VLSI VELOCITY SENSOR USING THE GRADIENT METHOD

Rainer A. Deutschmann and Christof Koch

139-74 California Institute of Technology
Pasadena, CA 91125, USA
rainer@klab.caltech.edu

ABSTRACT

Smart vision sensors that unify imaging and computation on one single chip offer great advantage over conventional sensor systems, where the computational part is usually performed separately and serially on a digital computer. Using parallel analog VLSI design principles, compact, low power, inexpensive and real time sensors can be built even in standard CMOS processes.

In this paper we present the first working analog VLSI implementation of a 1-D velocity sensor that uses the gradient method for spatially resolved velocity computation. We use a novel floating gate wide linear range amplifier and a floating gate division circuit. The division by zero problem of the gradient method has been solved. The sensor velocity output linearly codes the stimulus velocity over a wide range, is independent of contrast down to 20% contrast and indicates the correct direction-of-motion down to 4% contrast. In a circular pixel arrangement the sensor reports the rotational velocity up to 350 rpm.

1. INTRODUCTION

Moving scenes are a rich source of information. From the optical flow important parameters such as ego-motion, time-to-contact and the focus-of-expansion can be inferred. Tracking systems can use velocity information, and object segmentation and figure-ground segmentation based on edge detection can be improved by using discontinuities of the optical flow field.

Image velocity estimation has successfully been performed in software, but high frame rates require powerful computers. More recently VLSI systems have been developed where imaging and velocity computation are integrated on one single chip. There are two types of algorithms for determining the velocity field. In the *gradient method* the local velocity is obtained by dividing temporal and spatial derivatives of the local light intensity distribution, whereas in *correlation based methods* image features, such as intensity patterns or edges, are extracted and correlated.

R. D. is now at the Walter Schottky Institut, Technische Universität München, Am Coulombwall, 85748 Garching, GERMANY

Up to now no successful implementation of the gradient method has been reported. One of the earliest analog VLSI velocity chips [1] was supposed to solve the optical flow equation (see section 2), but due to the implementation of the algorithm only one global velocity vector could possibly be obtained.

Subsequently research has concentrated on correlation based methods for velocity estimation [2] [3] [4]. A successful class of sensors measures time of travel of a token [5] [6] [7].

In this paper we present the first analog VLSI sensor that computes the spatially resolved image velocity by a real time division of the temporal and spatial derivatives of the local light intensity. The algorithm is derived in the following section. In section 3 the implementation is described, and in section 4 experimental results are presented.

2. ALGORITHM

An equation which relates the change in image brightness at a point in a plane to the motion of the brightness pattern can be derived from the assumption, that the brightness of a particular point in the pattern is constant:

$$\frac{d}{dt}I(x, y, t) = 0 \Rightarrow \frac{\partial I}{\partial x}v_x + \frac{\partial I}{\partial y}v_y + \frac{\partial I}{\partial t} = 0, \quad (1)$$

where $I(x, y, t)$ is the image intensity on the focal plane and (v_x, v_y) the velocity vector.

From this equation one readily obtains by rearranging for one spatial dimension

$$v(x, t) = -\frac{\partial I / \partial t}{\partial I / \partial x}, \quad (2)$$

i.e. the local velocity can be computed from the division of the temporal and spatial derivatives. It can be seen that velocity information is obtained continuously in time as long as temporal and spatial changes are present. Token based methods, though, can only respond to specific features, and after detection the velocity information has to be stored.

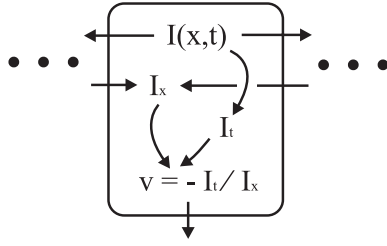


Figure 1: Blockdiagram of one pixel.

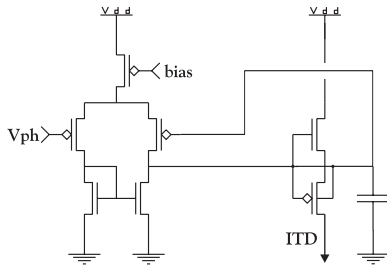


Figure 2: Temporal derivative circuit.

3. IMPLEMENTATION

Our implementation of equation 2 in analog VLSI hardware consists of four major building blocks, as shown in Figure 1: An adaptive photoreceptor [8], temporal and spatial derivative circuits, and a division circuit. The local light intensity $I(x, t)$ is used for the temporal derivative I_t and is fed to the neighbouring pixels for computing the spatial derivative I_x . The velocity v is obtained from a division of temporal and spatial derivatives.

The temporal derivative circuit (Figure 2) follows [9] and provides a current I_{td} proportional to the rate of change of the photoreceptor voltage V_{ph} for decreasing light intensities.

For the spatial derivative a new wide linear range amplifier was developed (Figure 3). The inputs are coupled to a differential pair through floating gate capacitive dividers. Neglecting parasitic capacitances, the linear range is increased by a factor $1 + C_{ref}/C$. This factor was chosen such that the current I_{sd} was linear in the voltage $V_{ph2} - V_{ph1}$ for all natural photoreceptor voltages.

The division circuit (Figure 4) was developed following translinear design principles [10]. The circuit involves only 4 transistors and one current source. Because the input currents can only be unidirectional, the spatial derivative current I_{sd} is rectified before the division (circuit not shown). The output current I_{div} is computed from I_{td} , I_{sd} and a reference current I_{mult} such that

$$I_{div} = I_{mult} \times \frac{I_{td}}{I_{sd}}. \quad (3)$$

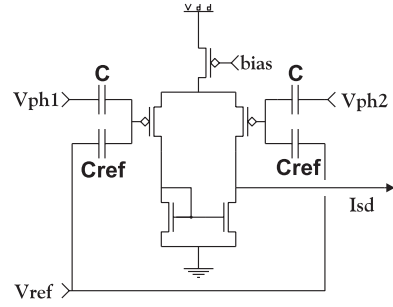


Figure 3: Wide linear range amplifier circuit.

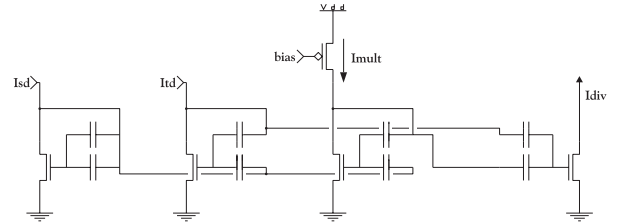


Figure 4: Division circuit.

as long as all currents stay subthreshold, i.e. $<100\text{nA}$. The sign of the velocity output current I_{div} is then corrected in a simple switching circuit (not shown).

We used a commercially available $2.0\mu\text{m}$ CMOS process. The pixel size was $147\mu\text{m} \times 270\mu\text{m}$ but can be optimised. On a $2.2\text{mm} \times 2.2\text{mm}$ chip we circularly arranged 20 pixels, each one of which could be accessed through an on-chip scanner. Besides a 5V power supply and a few bias voltages only a lens is required for operation.

4. RESULTS

For debugging reasons not only the computed velocity signal but also the photoreceptor voltage and the temporal and spatial derivatives can be accessed from each pixel. In Figure 5 these signals were recorded over time from one pixel while a moving sinusoidal gray value pattern was presented to the sensor. The top traces show the photoreceptor voltage together with the velocity output. The photoreceptor voltage reflects the sinusoidal stimulus. It can be seen that the sensor reports a constant stimulus velocity during the time when the temporal derivative is computed (falling light intensities), otherwise zero velocity is reported. The height of the plateau indicates the stimulus velocity. The fact that the sensor reports a constant velocity is remarkable considering that both temporal and spatial derivatives are varying according to the stimulus shape, as shown in the two lower traces. The spatial derivative matches the theoretical expectation (phase shifted rectified sinusoid), and the temporal

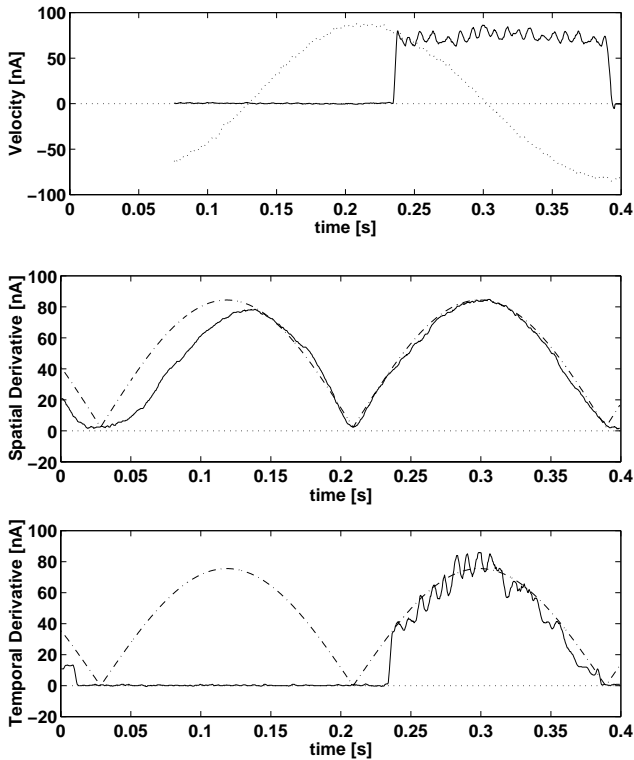


Figure 5: Velocity output and photoreceptor output (dotted) from one pixel for sinusoidal stimulus (top traces). Rectified spatial derivative (middle trace) and temporal derivative (bottom trace) with fit (dashed lines).

derivative is computed correctly as half wave sinusoid during falling intensities.

In Figure 6 the height of the plateau is plotted against the stimulus velocity from 2 mm/sec up to 76 mm/sec. A sine wave stimulus of 72.5% contrast and spatial frequency 0.05 cycles/deg was used. The reported velocity is almost linear with the stimulus velocity over the whole range. The errorbars represent one standard deviation on each side and were obtained over multiple presentations of the same stimulus. With one bias voltage set slightly different an almost linear relationship between stimulus velocity and reported velocity is also obtained for velocities as low as 0.07 mm/sec (almost invisible) up to 2 mm/sec. The same experiments have been performed with saw tooth stimuli and yielded the same linearity.

In Figure 7 the velocity output is plotted for a sinusoid stimulus of constant velocity but different contrasts. The velocity output is independent of the stimulus contrast over a wide range down to 20% contrast. For very small contrasts in order to avoid the division by zero problem in equation 2 a small current is added to the spatial derivative and a different current is subtracted from the temporal derivative. Therefore the velocity output approaches zero

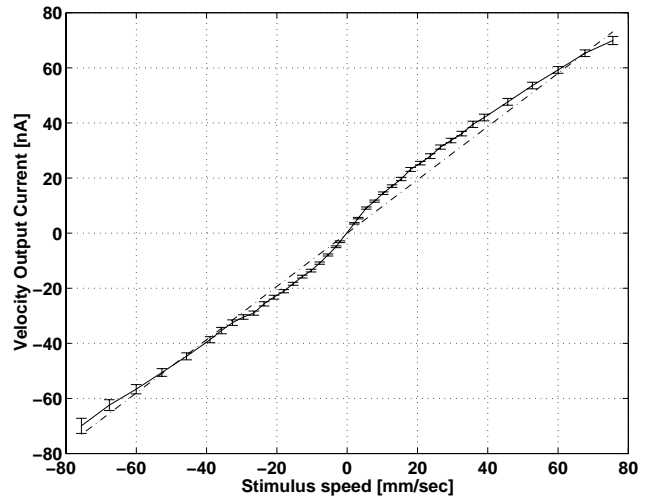


Figure 6: Velocity dependence.

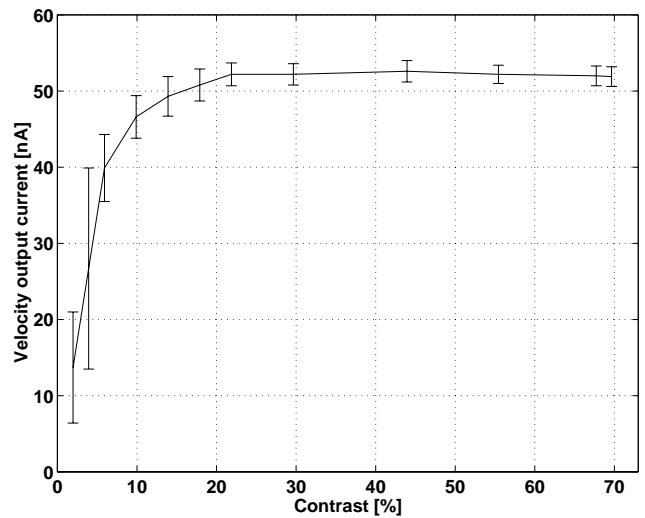


Figure 7: Contrast dependence.

for small contrasts. The correct direction-of-motion is reported down to contrast of 4%.

In the previous experiments only one pixel was read out at a time. In a different scanning mode the velocity outputs of all pixels can be summed together. No clock is then needed. If the pixels are arranged in a line, the global translatory velocity can robustly be detected. On one sensor chip we circularly arranged 25 pixels (see Figure 8), which allows for a robust measurement of the rotational velocity. Figure 9 shows the sensor output for a rotating stimulus: Up to 2120 deg/sec (353 rpm) the stimulus velocity is reported almost linearly.

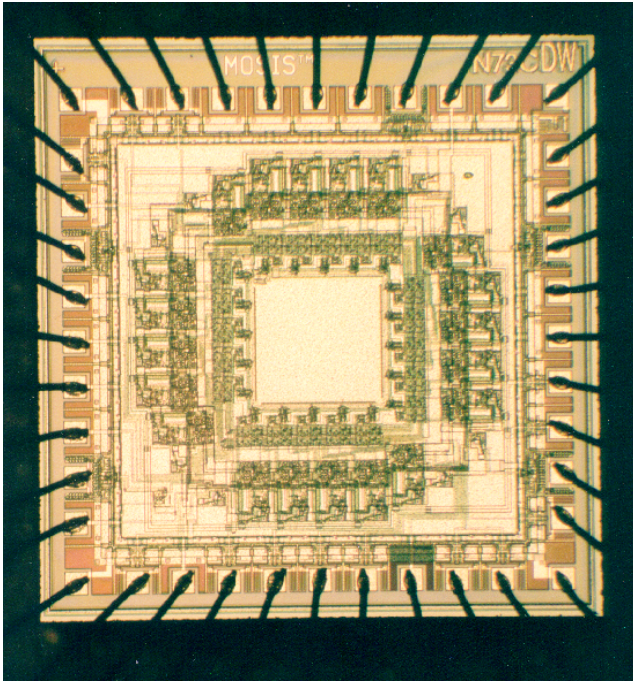


Figure 8: Micro photograph of the sensor chip.

5. DISCUSSION

The first analog CMOS sensor is presented that implements the gradient method for spatially resolved velocity computation. The sensor features a wide dynamic range, good linearity and robust operation. In a linear or circular pixel arrangement the sensor can additionally compute the global translatory or rotatory velocity, respectively. As predicted by the theory for a discrete implementation of the gradient method, the velocity output increases for spatial frequencies close to the Nyquist frequency. It is therefore desirable to further optimise the pixel size. Based on the circuits presented here the gradient method can be implemented for a 2-D velocity sensor.

6. ACKNOWLEDGEMENTS

This work was supported by the Center for Neuromorphic Systems Engineering as a part of the National Science Foundation's Engineering Research Center program.

7. REFERENCES

- [1] J. Tanner and C. Mead. "An integrated optical motion sensor". *VLSI Signal Processing II, IEEE Press*, pages 59–76, 1986.
- [2] A.G. Andreou, K. Strohhahn, and R.E. Jenkins. "Silicon retina for motion computation". *Proc. IEEE Int. Symp. on Circuits and Systems*, 3:1373–1376, 1991.

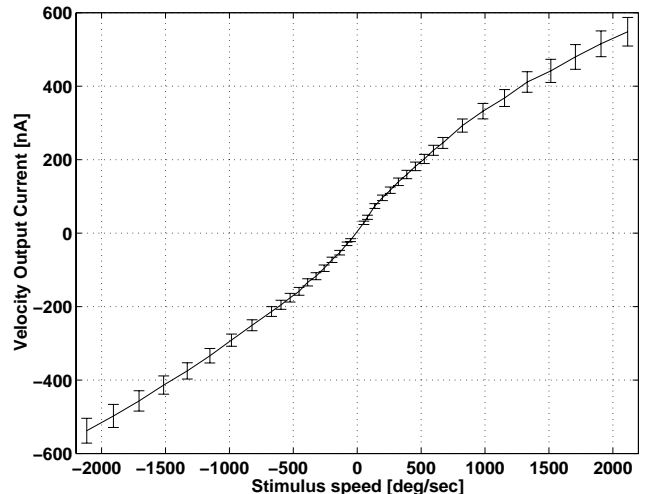


Figure 9: Measuring rotational velocity.

- [3] T. Delbrück. "Silicon retina with correlation-based, velocity-tuned pixels". *IEEE Trans. on Neural Networks*, 4:529–541, 1993.
- [4] T.K. Horiuchi, W. Bair, B. Bishofberger, A. Moore, and C. Koch. "Computing motion using analog VLSI vision chips: an experimental comparison among different approaches". *Intern. Journal of Computer Vision*, 8:203–216, 1992.
- [5] R. Etienne-Cummings, J. Van der Spiegel, and P. Mueller. "A focal plane visual motion measurement sensor". *IEEE Trans. Circuits and Systems I*, 44:55–66, 1997.
- [6] J. Kramer. "Compact integrated motion sensor with three-pixel interaction". *IEEE Trans. Pattern Anal. Machine Intell.*, 18:455–560, 1996.
- [7] J. Kramer, R. Sarpeshkar, and C. Koch. "Pulse-based analog VLSI velocity sensors". *IEEE Trans. Circuits and Systems II*, 44:86–101, 1997.
- [8] T. Delbrück and C. Mead. "Analog VLSI Phototransduction". *CNS Memo No.30, Caltech*, pages 139–161, 1994.
- [9] T. Horiuchi. "Analog VLSI-based, neuromorphic sensorimotor systems: modeling the primate oculomotor system". *California Institute of Technology, PhD Thesis*, 1997.
- [10] B. A. Minch, C. Diorio, P. Hasler and C. Mead. "Translinear Circuits using subthreshold floating-gate MOS-transistors". *Analog Integrated Circuits and Signal Processing*, 9:167–179, 1996.